

1 Determination of respiration and photosynthesis fractionation factors  
2 for atmospheric dioxygen inferred from a vegetation-soil-atmosphere  
3 analog of the terrestrial biosphere in closed chambers

4

5 Clémence Paul<sup>1</sup>, Clément Piel<sup>2</sup>, Joana Sauze<sup>2</sup>, Nicolas Pasquier<sup>1</sup>, Frédéric Prié<sup>1</sup>, Sébastien Devidal<sup>2</sup>,  
6 Roxanne Jacob<sup>1</sup>, Arnaud Dapoigny<sup>1</sup>, Olivier Jossoud<sup>1</sup>, Alexandru Milcu<sup>2,3</sup>, Amaëlle Landais<sup>1</sup>

7

8 <sup>1</sup>Laboratoire des Sciences du Climat et de l'Environnement, LSCE/IPSL, CEA-CNRS-UVSQ, Université Paris-  
9 Saclay, 91191 Gif-sur-Yvette, France

10 <sup>2</sup>Ecotron Européen de Montpellier (UAR 3248), Univ Montpellier, Centre National de la Recherche Scientifique  
11 (CNRS), Campus Baillarguet, Montferrier-sur-Lez, France

12 <sup>3</sup>Centre d'Ecologie Fonctionnelle et Evolutive, Univ Montpellier, CNRS, Univ Paul Valéry, EPHE, IRD, Montpellier,  
13 France

14

15 Correspondence: Clémence Paul (clemence.paul@lsce.ipsl.fr)

16

17 Abstract

18 The isotopic composition of dioxygen in the atmosphere is a global tracer which depends on the  
19 biosphere flux of dioxygen toward and from the atmosphere (photosynthesis and respiration) as well  
20 as exchanges with the stratosphere. When measured in fossil air trapped in ice cores, the relative  
21 concentration of <sup>16</sup>O, <sup>17</sup>O and <sup>18</sup>O of O<sub>2</sub> can be used for several applications such as ice core dating and  
22 past global productivity reconstruction. However, there are still uncertainties about the accuracy of  
23 these tracers as they depend on the integrated isotopic discrimination of different biological processes  
24 of dioxygen production and uptake, for which we currently have very few independent estimates.  
25 Here we determined the respiration and photosynthesis fractionation factors for atmospheric  
26 dioxygen from experiments carried out in a replicated vegetation-soil-atmosphere analog of the  
27 terrestrial biosphere in closed chambers with growing *Festuca arundinacea*. The values for <sup>18</sup>O  
28 discrimination during soil respiration and dark respiration in leaves are equal to  $-12.3 \pm 1.7$  ‰ and  $-$   
29  $19.1 \pm 2.4$  ‰, respectively. We also found a value for terrestrial photosynthetic isotopic discrimination  
30 equal to  $+3.7 \pm 1.3$  ‰. This last estimate suggests that the contribution of terrestrial productivity in  
31 the Dole effect may have been underestimated in previous studies.

32

## 33 1. Introduction

34 The oxygen cycle represents one of the most important biogeochemical cycles on Earth as oxygen is  
35 the second most important gaseous component in the atmosphere. Oxygen is an essential component  
36 for life on Earth as it is consumed by all aerobic organisms through respiration and produced by  
37 autotrophic organisms through photosynthesis.

38 The analysis of the oxygen isotopic composition classically expressed as  $\delta^{18}\text{O}$  and  $\delta^{17}\text{O}$  of  $\text{O}_2$  in air  
39 bubbles trapped in ice cores is currently used to provide information on the variations of the low  
40 latitude water cycle and the productivity of the biosphere during the Quaternary (Bender et al., 1994;  
41 Luz et al., 1999; Malaizé et al., 1999; Severinghaus et al., 2009; Blunier et al., 2002; Landais et al., 2010).  
42  $\delta^{18}\text{O}$  of  $\text{O}_2$  is also a very useful proxy for ice core dating through the resemblance of its variations with  
43 the variations of precession or summer insolation in the northern hemisphere (Shackleton, 2000;  
44 Dreyfus et al., 2007). These tracers are however complex and their interpretation relies on the precise  
45 knowledge of the various fractionation factors in the oxygen cycle.

46 First, interpreting the relationship between  $\delta^{18}\text{O}$  of  $\text{O}_2$  (or  $\delta^{18}\text{O}_{\text{atm}}$ ) variations in ice core air and the low  
47 latitude water cycle (e.g. Severinghaus et al., 2009; Landais et al., 2010; Seltzer et al., 2017) is still  
48 debated because of the multiple processes involved. Dole et al. (1954) showed that  $\delta^{18}\text{O}_{\text{atm}}$  is enriched  
49 compared to the  $\delta^{18}\text{O}$  of water of the global ocean (taken here as the Vienna Standard Mean Ocean  
50 Water, VSMOW) with a value of 23.88 ‰ (Barkan and Luz, 2005). This Dole effect is the result of several  
51 isotopic discriminations caused by biotic processes that enrich the  $\delta^{18}\text{O}_{\text{atm}}$  relative to the oceanic  
52 values of water  $\delta^{18}\text{O}$ . First measurements have shown that the photosynthesis itself is not associated  
53 with a strong isotopic discrimination and produces oxygen with an isotopic composition which is close  
54 to the isotopic composition of the consumed water (Vinogradov et al., 1959; Stevens et al., 1975; Guy  
55 et al., 1993; Helman et al., 2005; Luz & Barkan, 2005). This is in contrast to the early results of Dole  
56 and Jenks (1959) who proposed a photosynthetic isotopic discrimination for plants and algae of 5‰.  
57 Vinogradov et al. (1959) challenged the results of Dole and Jenks (1944) by explaining that the  $^{18}\text{O}$   
58 enrichment of  $\text{O}_2$  during their photosynthesis experiments is the result of contamination by  
59 atmospheric  $\text{O}_2$  and respiration. Guy et al. (1993) studied the photosynthetic isotopic discrimination  
60 on spinach thylakoids, cyanobacteria (*Anacystis nidulans*) and diatoms (*Phaeodactylum tricornutum*)  
61 and found only a slight isotopic discrimination of 0.3‰ which they considered negligible. Luz and  
62 Barkan (2005) also corroborates this idea by studying photosynthetic isotopic discrimination on  
63 Philodendron and did not obtain a  $^{18}\text{O}$  enrichment of the  $\text{O}_2$  produced. This absence of isotopic  
64 discrimination can be theoretically explained by the process of  $\text{O}_2$  generation within photosynthesis  
65 (photosystem II) involving water oxidation by the oxygen evolving complex (Tcherkez and Farquhar,

66 2007). For the oceanic biosphere, the isotopic composition of O<sub>2</sub> produced by photosynthesis is very  
67 close to the isotopic composition of the ocean. However, in terrestrial biosphere the δ<sup>18</sup>O of water  
68 split during photosynthesis (leaf water) is highly variable both spatially and temporally because of the  
69 decrease of δ<sup>18</sup>O of meteoric water toward higher latitudes (Dansgaard, 1974) and the enrichment in  
70 heavy isotopes in leaf water during evaporation (Dongmann et al., 1974). The mean δ<sup>18</sup>O enrichment  
71 of leaf water isotopic composition has been estimated between + 4.5 and + 6 ‰ with respect to the  
72 isotopic composition of mean global ocean water (Bender et al., 1994; Hoffmann et al., 2004). On top  
73 of this enrichment, the terrestrial and oceanic Dole effects are mostly explained by the respiratory  
74 isotopic discrimination of the order of magnitude of + 18 ‰ (Bender et al., 1994).

75 Because of the isotopic enrichment in leaf water, the terrestrial Dole effect has been initially estimated  
76 to be 5 ‰ higher than the oceanic Dole effect and δ<sup>18</sup>O<sub>atm</sub> used to estimate changes in the balance  
77 between land and marine productivity (Wang et al., 2008; Bender et al., 1994; Hoffmann et al., 2004).  
78 However, the evidence by Eisenstadt et al. (2010) of isotopic discrimination up to + 6‰ for marine  
79 phytoplankton photosynthesis rather suggests that the marine and terrestrial Dole effects are of the  
80 same order of magnitude. More specifically, Eisenstadt et al. (2010) determined several  
81 photosynthetic isotopic discrimination values depending on the phytoplankton studied  
82 (*Phaeodactylum tricornutum* = 4.5 ‰, *Nannocloreopsis sp.* = 3 ‰, *Emiliana huxleyi* = 5.5 ‰ and  
83 *Chlamydomonas oreinhardtii* = 7 ‰). If marine and terrestrial Dole effects are similar, then the past  
84 variations of δ<sup>18</sup>O<sub>atm</sub> cannot be attributed to different proportions of terrestrial or marine Dole effects.  
85 They would better be related to low latitude water cycle influencing the leaf water δ<sup>18</sup>O consumed by  
86 photosynthesis and then the δ<sup>18</sup>O of O<sub>2</sub> produced by this process (with a larger flux in the low latitude  
87 vegetated regions). This is supported by orbital and millennial variations of δ<sup>18</sup>O<sub>atm</sub> in phase with calcite  
88 δ<sup>18</sup>O in Chinese speleothem, a proxy strongly related to the intensity of hydrological cycle in the South-  
89 East Asia (Severinghaus et al., 2009; Landais et al., 2010; Extier et al., 2018). The aforementioned  
90 studies show that qualitative and quantitative interpretation of δ<sup>18</sup>O<sub>atm</sub> relies strongly on the estimate  
91 of O<sub>2</sub> fractionation factors in the biological cycle but data to constrain the fractionation factors  
92 associated with respiration and photosynthesis for the different ecosystems are sparse.

93 In addition to the use of δ<sup>18</sup>O<sub>atm</sub>, the combination of δ<sup>17</sup>O and δ<sup>18</sup>O of O<sub>2</sub> provides a way to quantify  
94 variations in past global productivity (Luz et al., 1999). This method relies on the fact that O<sub>2</sub>-  
95 fractionating processes in the stratosphere and within the biosphere lead to different relationships  
96 between δ<sup>17</sup>O and δ<sup>18</sup>O of O<sub>2</sub>. Oxygen is fractionated in a mass-independent manner in the  
97 stratosphere producing approximately equal <sup>17</sup>O and <sup>18</sup>O enrichments (Luz et al., 1999). On the  
98 contrary, the biosphere fractionating processes are mass-dependent such that the <sup>17</sup>O enrichment is  
99 about half the <sup>18</sup>O enrichment relative to <sup>16</sup>O. We thus define a Δ<sup>17</sup>O anomaly as:

100

$$101 \quad \Delta^{17}O = \ln(1 + \delta^{17}O) - 0.516 \times \ln(1 + \delta^{18}O) \quad (1)$$

102

103  $\Delta^{17}O$  of  $O_2$  is equal to 0 by definition in the present-day troposphere (the standard for isotopic  
104 composition of atmospheric oxygen is the present-day atmospheric value).  $\Delta^{17}O$  of  $O_2$  is negative in  
105 the stratosphere and increases in biosphere productivity leads to an increase of  $\Delta^{17}O$  of  $O_2$ . As for the  
106 interpretation of  $\delta^{18}O_{atm}$ , the quantitative link between  $\Delta^{17}O$  of  $O_2$  and biosphere productivity depends  
107 on the exact fractionation factors associated with biosphere processes (Brandon et al., 2020).

108 Several studies have been conducted to estimate the fractionation factors during biosphere processes  
109 of  $O_2$  production and consumption. These fractionation factors are then implemented in global  
110 modeling approaches involving the use of models of global vegetation and oceanic biosphere for  
111 interpretation of  $\Delta^{17}O$  of  $O_2$  and  $\delta^{18}O_{atm}$  in term of environmental parameters (Landais et al., 2007;  
112 Blunier et al., 2012; Reutenauer et al., 2015; Brandon et al., 2020). Most of the fractionation factors  
113 used in these modeling approaches were obtained from studies conducted at the cell level:  
114 cyanobacterium (Helman et al., 2005), *E. coli* (Stolper et al., 2018), microalgae (Eisenstadt et al., 2010).  
115 In these studies, the underlying assumption is that the fractionation factor associated with  $O_2$   
116 measured at the cell level can be applied at the ecosystem scale. Yet, results from studies conducted  
117 at a larger scale, e.g. at the soil scale by Angert et al. (2001) found a global terrestrial respiratory  
118  $^{18}O/^{16}O$  of  $O_2$  discrimination for soil microorganisms varying between - 12 ‰ and - 15 ‰. This is lower  
119 than the - 18 ‰ discrimination classically used for respiration, with diffusion in soil playing a role in  
120 addition to the biological respiration isotopic discrimination. Angert and Luz (2001) also showed using  
121 experiments on roots of *Philodendron* plants and wheat seedlings that the respiratory discrimination  
122 of a soil with roots is lower (about - 12‰) than the - 18‰ discrimination associated with the dark  
123 respiration. This is due to the low  $O_2$  concentration in roots whose presence favors a slower diffusion.  
124 Later, Angert et al. (2003) found an even larger spread of  $O_2$  isotopic discrimination in soil and showed  
125 that temperate and boreal soils have higher isotopic discrimination, respectively - 17.8 ‰ and -  
126 22.5 ‰.

127 It has been suggested that the strong discrimination observed for boreal and temperate soils is due to  
128 the involvement of the alternative oxidase pathway (AOX, Bendall and Bonner, 1971) in addition to  
129 the usual COX respiratory pathway. In the COX respiration pathway, present in the majority in plants,  
130 the cytochrome oxidase enzyme catalyzes the oxygen reduction reaction. In the AOX pathway, the  
131 oxidation of ubiquinol molecules is directly coupled to the reduction of oxygen. Guy et al. (2005)  
132 showed that, for green tissues, the respiratory discrimination of the AOX pathway is much higher (-

133 31‰) than the one of the COX pathway (- 21‰). Similarly, Ribas-Carbo et al. (1995) found a higher  
134 respiratory discrimination in phytoplankton that engage the AOX pathway (- 31 ‰) relative to bacteria  
135 that engage the COX pathway (- 24 ‰).

136 Other studies had attempted to investigate the different respiratory discriminations in the light (dark  
137 respiration, Mehler reaction and photorespiration). As during the light period, dark respiration can be  
138 inhibited (70 % inhibition found by Tcherkez et al. (2017) and Keenan et al. (2019)), so that the other  
139 O<sub>2</sub> consuming processes are important to consider. The Mehler reaction reduces oxygen to form a  
140 superoxide ion which is converted to hydrogen peroxide (H<sub>2</sub>O<sub>2</sub>) in photosystem I and then further  
141 converted to water (Mehler, 1951). Photorespiration is the result of the oxygenase activity of Rubisco  
142 (Sharkey, 1998). This enzyme can oxidize ribulose-1,5-bisphosphate with an oxygen molecule O<sub>2</sub>. This  
143 reaction causes a loss of CO<sub>2</sub> incorporation, thus decreasing the photosynthetic yield (Bauwe et al.,  
144 2010). Guy et al. (1993) first found a photorespiratory discrimination of - 21.7 ‰ and a <sup>18</sup>O/<sup>16</sup>O  
145 discrimination of - 15.3 ‰ for the Mehler reaction. Later, on a study performed on pea, Helman et al.  
146 (2005) found <sup>18</sup>O/<sup>16</sup>O discriminations of - 21.3 ‰ and - 10.8 ‰ respectively for photorespiration and  
147 Mehler reaction.

148 The above presented state of the art shows contrasting results for the determination of fractionation  
149 factors for the different photosynthesis and O<sub>2</sub> uptake processes, thus underlining the importance of  
150 performing new measurements to correctly interpret global variations of the isotopic composition of  
151 oxygen. Moreover, because there may be a difference between the fractionation factors at the cell  
152 level and at a broader level as shown for dark respiration in soil, we will favor here an approach at the  
153 scale of a terrarium including plant and soil.

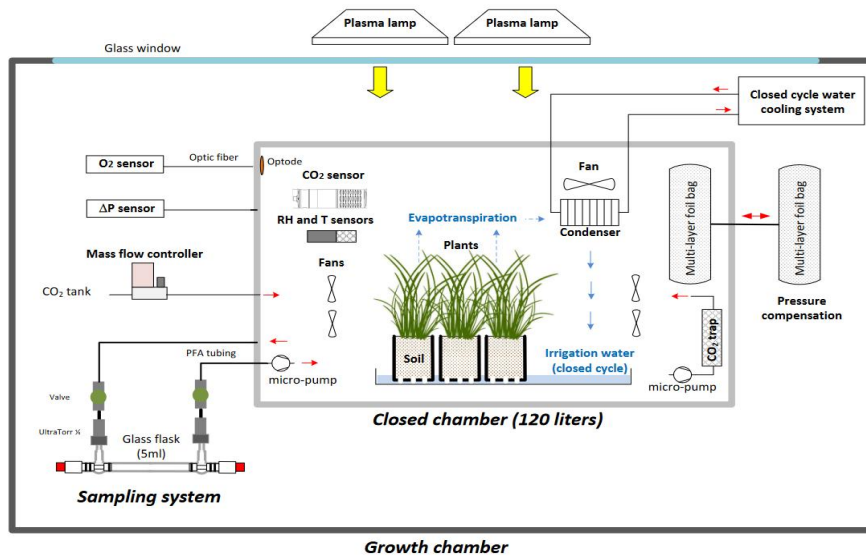
154 In this study we developed a simplified vegetation-soil-atmosphere analog of the terrestrial biosphere  
155 in closed chamber of 120 dm<sup>3</sup> with the aim of estimating the fractionation factors of atmospheric  
156 dioxygen due to soil respiration, plant respiration and photosynthesis. With this setup we carried out  
157 several experimental runs with soil only and soil with plants in order to estimate the isotopic  
158 discrimination of the different compartments and check values obtained at the cell level. The  
159 implications for our interpretation of the Dole effect are also discussed.

## 160 2. Material and Methods

### 161 2.1. Growth chamber and closed system

#### 162 2.1.1. Plant growth and experimental setup

##### 163 a)



164

165 b)



166

167 **Fig.1. A vegetation-soil-atmosphere analog of the terrestrial biosphere in a closed chamber. (a)**  
 168 **Schematic of the closed chamber setup used for the terrestrial biosphere model.** The 120 dm<sup>3</sup> gas  
 169 tight closed chamber containing a terrestrial biosphere analogue is enclosed in a larger growth  
 170 chamber from the Ecotron Microcosms platform. Main environmental parameters inside the closed  
 171 chamber are actively controlled and monitored: temperature (T), light intensity, CO<sub>2</sub>, relative humidity  
 172 (RH), pressure differential (ΔP). The water cycle in the closed chamber is shown in blue. **(b) Photograph**  
 173 **of the closed chamber used in the experiment with *Festuca arundinacea*.**

174

175 Seeds of *Festuca arundinacea* (Schreb.), also commonly called tall fescue, were first sown in a  
 176 commercial potting soil (Terreau universel, Botanic, France. Composition: black and blond peat, wood

177 fibre, green compost and vermicompost manure, organic and organo-mineral fertilizers and  
178 micronutrient fertilizers). During 15 to 20 days, they were then placed in a growth chamber of the  
179 Microcosms experimental platform of the European Ecotron of Montpellier  
180 (<https://www.ecotron.cnrs.fr>) under diurnal light-dark cycles (Table S1), air temperature set at 20 °C  
181 ( $T_{\text{air}}$ ), air relative humidity (RH) at 80 % and CO<sub>2</sub> atmospheric concentration close to ambient air  
182 (concentration of CO<sub>2</sub> = 400 ppm).

183 Twelve pots (8 cm × 8 cm × 12 cm with 180 to 200 g of dry soil) containing approximately 25 to 30  
184 mature fescue plants were used for each experimental run. All plants were placed in a plastic tray filled  
185 with tap water, inside an airtight transparent chamber manufactured from welded polycarbonate (10  
186 mm wall thickness and 120 liters volume) similar to the chambers used by Milcu et al. (2013) (Fig. 1).  
187 The sealing of the closed chamber was checked before each experiment using helium.

188 To control temperature and light intensity inside the closed chamber, this smaller chamber was placed  
189 in a larger controlled environment growth chamber. Light was provided by two plasma lamps (GAVITA  
190 Pro 300 LEP02; GAVITA) with PAR = 200  $\mu\text{mol}\cdot\text{m}^{-2}\cdot\text{s}^{-1}$  and air temperature inside the closed chamber  
191 was regulated at  $19 \pm 1$  °C by adjusting the growth chamber temperature.

192 The closed chamber (Fig. 1) was used as a closed gas exchange system with controlled, and  
193 continuously monitored, environmental parameters. Air and soil temperature (CTN 35, Carel), air  
194 relative humidity (PFmini72, Michell instrument, USA) and CO<sub>2</sub> atmospheric concentration (GMP343,  
195 Vaisala, Finland) were measured and recorded using the growth chamber datalogger (sampling rate =  
196 1 min). O<sub>2</sub> concentration was continuously monitored using an optical sensor (Oxy1-SMA, Presens,  
197 Germany). Because precise O<sub>2</sub> concentration are determined in our samples by mass spectrometry  
198 (see next section), the measurements of the Oxy1-SMA were only used as a control during the  
199 experiment. The measured O<sub>2</sub> value for atmospheric air was adjusted to 20.9 % before each sequence  
200 of experiments and the same adjustment (offset) was then applied to the O<sub>2</sub> record during the  
201 following sequence.

202 Air relative humidity was regulated between 80 % and 90 % using a heat exchanger (acting as a  
203 condenser) connected to a closed cycle water cooling system. The condenser was positioned in a way  
204 to create a closed water cycle in the biological chamber (water vapor from evapotranspiration was  
205 condensed back into irrigation water). In order to keep the CO<sub>2</sub> mixing ratio close to 400 ppm during  
206 the light periods, photosynthetic CO<sub>2</sub> uptake was compensated with injections of pure CO<sub>2</sub> using a  
207 mass flow controller (F200CV, Bronkhorst, The Netherlands). During the dark periods, a soda lime trap  
208 connected to a micro-pump (NMS 020B, KNF, Germany) was used to remove the excess CO<sub>2</sub> coming  
209 from respiration. CO<sub>2</sub> atmospheric concentration during the night was kept below 200 ppm.

210 To ensure atmospheric pressure stability in the closed chamber, a pressure compensation system,  
211 made of two connected 10 liters gas tight bags (Restek multi-layer polyvinyl fluoride foil gas sampling

212 bag, USA), was installed. Each bag was half full of atmospheric air, the first one was installed in the  
213 closed chamber while the second one was outside this chamber. This way, each bag inflated or deflated  
214 in response to pressure variations caused either by O<sub>2</sub> or CO<sub>2</sub>, uptake or release. The pressure  
215 difference between the closed chamber and the atmosphere was regularly measured using a  
216 differential sensor (FD A602-S1K Almemo, Ahlborn, Germany).

217 Finally, the enclosed air was mixed and considered homogeneous using seven brushless fans.

218

### 219 **2.1.2. Gas sampling**

220

221 To measure the isotopic composition along the experiment, small samples of gas were collected in 5  
222 mL glass flasks, made of two Louwers H.V. glass valves (1-way bore 9mm Ref. LH10402008, Louwers  
223 Hanique, The Netherlands) welded together. Those flasks, previously evacuated, were mounted on  
224 PFA tubing (1/4<sup>th</sup>) using two 1/4<sup>th</sup> UltraTorr fitting (SS-4-UT-9, Swagelok, USA). Two manual valves (SS-  
225 4H, Swagelok, USA) were also installed on the PFA tubes to open or close the circuit. A micro-pump  
226 (NMS 20B, KNF, Germany) was finally turned on during air sampling to ensure closed chamber  
227 atmosphere circulation through the flask. The flow rate was equal to 1.6 L/min.

228

## 229 **2.2. Isotopic measurements**

### 230 **2.2.1. Water extraction from leaf and isotopic analysis**

231 After each experiment, the plant leaves were collected, placed in airtight flasks and immediately frozen  
232 at - 20°C for at least 24 hours to make sure there was minimal loss of water through vaporization when  
233 the vial was opened later. The extraction of water from leaves was done according to the procedure  
234 detailed in Alexandre et al. (2018). The vial was fixed onto a cryogenic extraction line and was first  
235 immersed in a liquid nitrogen Dewar to prevent any sublimation of the water. The water extraction  
236 line was emptied of most of its air (< 10<sup>-5</sup> Pa). Once this pressure was reached, the pump was turned  
237 off and a valve was closed in order to keep a constant static void within the system. The “reception”  
238 vial was then immersed in a liquid nitrogen Dewar which will act as a water trap whilst the sample vial  
239 for the water was then transferred to a water bath maintained at 75°C. The system was kept in these  
240 conditions for no less than six hours, so that all the water present in the leaf and stems was extracted.  
241 Afterwards, in order to remove all of the organic compounds of the extracted water, an active charcoal  
242 was placed in the extracted water and left under agitation for the night.

243 For analysis of δ<sup>17</sup>O and δ<sup>18</sup>O of water, leaf water was converted to O<sub>2</sub> using a fluorination line for  
244 reaction of H<sub>2</sub>O with CoF<sub>3</sub> heated to 370°C at LSCE. The isotopic composition of the dioxygen was



245 measured an IRMS equipped with dual inlet (Thermo Scientific MAT253 mass spectrometer). The  
246 standard that was chosen was an O<sub>2</sub> standard calibrated against VSMOW. The precision was 0.015 ‰  
247 for δ<sup>17</sup>O, 0.010 ‰ for δ<sup>18</sup>O and 6 ppm for Δ<sup>17</sup>O (Eq. (1)), for more details, refer to Landais et al. (2006).  
248 The values of δ<sup>18</sup>O and δ<sup>17</sup>O of leaf water measured with respect to VSMOW are then expressed with  
249 respect to the isotopic composition of dioxygen in atmospheric air (classical standard for δ<sup>18</sup>O and δ<sup>17</sup>O  
250 of O<sub>2</sub> measurements). No consensus has been reached for the values of δ<sup>18</sup>O and δ<sup>17</sup>O of O<sub>2</sub> in  
251 atmospheric air with respect to δ<sup>17</sup>O and δ<sup>18</sup>O of H<sub>2</sub>O of VSMOW. These differences are most probably  
252 to be attributed to the different analytical techniques used for preparing and measuring the samples  
253 (Yeung et al., 2018; Wostbrock et al., 2021). In our case, because we use a similar set-up with the one  
254 developed by Barkan and Luz (2003) for the analyses of the triple isotopic composition of O<sub>2</sub> in air (cf  
255 next section), we have chosen to base our calculation on their estimates. In this study, we have thus  
256 chosen the value of 23.88 ‰ for δ<sup>18</sup>O of O<sub>2</sub> values with respect to VSMOW following (Barkan and Luz,  
257 2005). As for the δ<sup>17</sup>O of O<sub>2</sub> value with respect to VSMOW value, we use two different possible  
258 estimates from these authors, either 12.03 ‰ (Luz and Barkan, 2011) or 12.08 ‰ (Barkan and Luz,  
259 2005). We acknowledge that because of the absence of consensus, slightly different values could be  
260 obtained for the fractionation factors determined in this study if a different choice is made for the  
261 reference values of δ<sup>18</sup>O and δ<sup>17</sup>O of O<sub>2</sub> in atmospheric air with respect to δ<sup>17</sup>O and δ<sup>18</sup>O of H<sub>2</sub>O of  
262 VSMOW.

### 263 **2.2.2. O<sub>2</sub> purification and isotopic analysis**

264 The air samples collected in the closed chambers were transported to LSCE for analyses of the isotopic  
265 composition of O<sub>2</sub>. The flasks were connected on a semi-automatic separation line inspired from  
266 Barkan and Luz (2003) which was made up of 8 ports in which 2 standards (outside air) and 6 samples  
267 were analyzed daily (Brandon et al., 2020). After pumping the whole line, the air was circulated through  
268 a water trap (ethanol at - 100°C) and then through a carbon dioxide trap immersed in liquid nitrogen  
269 at - 196 °C. After collection of the gas samples on a molecular sieve trap cooled at - 196 °C, a helium  
270 flow carried it through a chromatographic column which was immersed in a water reservoir at 0 °C to  
271 separate the dioxygen and the argon from the dinitrogen. After separation of the dioxygen and argon  
272 from helium, the gas was collected in a stainless-steel manifold immersed in liquid helium at - 269 °C.  
273 After collection, the samples were analyzed by the IRMS previously mentioned for leaf water analyses.  
274 The following ratios were measured: <sup>18</sup>O/<sup>16</sup>O, <sup>17</sup>O/<sup>16</sup>O and O<sub>2</sub>/Ar (as an indicator of the O<sub>2</sub>  
275 concentration because Ar is an inert gas). δ<sup>17</sup>O and δ<sup>18</sup>O of O<sub>2</sub> each sample were obtained through 3  
276 series of 24 dual inlet measurements against a standard made of O<sub>2</sub> and Ar. This sequence was  
277 followed by 2 peak jumping analyses of the O<sub>2</sub>/Ar ratio including separate measurements of the O<sub>2</sub> and

278 Ar signals for both the standard and the sample. The uncertainty associated with each measurement  
279 was obtained from the standard deviation of the three runs and from the repeated peak jumping  
280 measurement for  $\delta O_2/Ar$  which was defined by  $\left[ \frac{\left( \frac{n(O_2)}{n(Ar)} \right)_{sample}}{\left( \frac{n(O_2)}{n(Ar)} \right)_{standard}} - 1 \right] * 1000$ , and  $n(O_2)$  is the  
281 number of moles of  $O_2$  and  $n(Ar)$  the number of moles of  $Ar$ . The uncertainty values for  $\Delta^{17}O$ ,  $\delta^{18}O$   
282 and  $\delta O_2/Ar$  were respectively 10 ppm, 0.05 ‰ and 0.5 ‰.

283 Each day, we performed measurements of the dioxygen isotopic composition and  $O_2/Ar$  ratio on two  
284 samples of outside air which is the standard for the isotopic composition of  $O_2$  (Hillaire-Marcel et al.,  
285 2021). So that the calibrated  $\delta^{18}O$  value for our sample was calculated as in equation 2:

286

$$287 \quad \delta^{18}O_{calibrated} = \left[ \frac{(\delta^{18}O_{measured}/1000)+1}{(\delta^{18}O_{outsideair}/1000)+1} - 1 \right] \times 1000 \quad (2)$$

288

## 289 **2.3. Experimental runs**

### 290 **2.3.1. General strategy**

291 Our goal was to calculate the fractionation factor associated with  $\delta^{17}O$  and  $\delta^{18}O$  for soil respiration,  
292 dark leaf respiration and photosynthesis using the microcosm described above. In order to quantify  
293 the fractionation factors, we needed to work in closed and controlled conditions. Given the volume of  
294 the closed chamber (120 dm<sup>3</sup>, hence about 1.12 moles of  $O_2$ ) and the order of magnitude of dark  
295 respiration (order of magnitude of 0.08  $\mu\text{mol } O_2 \text{ s}^{-1}$  for soil respiration) and net photosynthetic fluxes  
296 (order of magnitude of 0.45  $\mu\text{mol } O_2 \text{ s}^{-1}$ ) inside the chamber, we calculated that experiments should  
297 last from 3 days to more than 2 weeks so that more than one tenth of the  $O_2$  in the chamber can be  
298 recycled by the plant and soil. This recycling allows the creation of sufficiently large isotopic signals  
299 (especially  $\Delta^{17}O$  of  $O_2$ ) to be detected and measured. We set up two different experiments in the closed  
300 chamber, each experiment being repeated 3 or 4 times to characterize the experimental repeatability  
301 of the system.

302 The first experiment (repeated 4 times, i.e. in 4 sequences) aimed at studying the fractionation factors  
303 during soil respiration. The second experiment (repeated 3 times, i.e. in 3 sequences, each sequence  
304 being divided into several periods with or without light) aimed at studying the fractionation factors  
305 during dark respiration and photosynthesis of plants.

306 Prior to the aforementioned experiments, measurements were carried out on a closed empty chamber  
307 to check the absence of leaks as well as the absence of isotopic fractionation (Table S2).

308

### 309 **2.3.2. Soil respiration experiment**

310 To conduct the soil respiration experiment, 2.6 kg of soil (*Terreau universel, Botanic*) were placed in 12  
311 different pots. The light was turned off during this experimental run (Table S1). We decided not to  
312 apply any diurnal cycles during dark respiration experimentations for two reasons. First, we wanted to  
313 prevent the development of algae, mosses or any photosynthetic organisms in the chamber. Secondly,  
314 it was easier to optimize temperature control as the light radiation could increase the temperature  
315 inside the closed chamber. During this dark period, CO<sub>2</sub> from soil respiration accumulates in the  
316 biological closed chamber. To have a stable concentration of CO<sub>2</sub> during the whole dark period, the  
317 CO<sub>2</sub> was trapped using soda lime. Four sequences were performed with respective durations of 53, 51,  
318 43 and 36 days.

319

### 320 **2.3.3. Photosynthesis and dark respiration experiment**

321 We used the same soil with plants (*Festuca arundinacea*) grown before the start of the three  
322 sequences of the photosynthesis and dark respiration experiment. In order to obtain a significant  
323 change of the  $\Delta^{17}\text{O}$  of O<sub>2</sub> signal in our closed 120 dm<sup>3</sup> chambers, the 3 experiments were run for 1 to  
324 2 months. CO<sub>2</sub> level was controlled to 400 ppm by a CO<sub>2</sub> trap and CO<sub>2</sub> injections. This was done to  
325 ensure that the CO<sub>2</sub> in the chamber did not reach levels too far from the atmospheric composition as  
326 this could have affected the physiology of the plant. This could have affected the physiology of the  
327 plant. The light cycle was controlled to alternate between day (photosynthesis and respiration) and  
328 night conditions (respiration) (Table S1).

329 The values of the leaf water measurements are presented in supplementary Table S3. Because the  
330 experiments had to be carried in a closed chamber, we could not sample leaves during the experiment  
331 and only got a value at the end of each sequence. Nevertheless, we could compare the isotopic  
332 composition of the irrigation and soil water at the start and at the end of the experiment.

333

## 334 **2.4. Quantification of fractionation factors**

335 We detail below how we used the results from our experiments to quantify the associated  
336 fractionation factors. Notations used below are gathered in Table 1.

337 The isotopic fractionation factor of oxygen is expressed through the fractionation factor  $\alpha$ .

338

$$339 \quad {}^{18}\alpha = \frac{{}^{18}R_{product}}{{}^{18}R_{substrat}} \quad (3)$$

340

341 where  $\alpha$  is the fractionation factor and  ${}^{18}R$  is the ratio of the concentration  ${}^{18}R = \frac{n({}^{18}O)}{n({}^{16}O)}$  with  $n$  the  
342 number of moles of  $O_2$  containing  ${}^{18}O$  or  ${}^{16}O$ .  ${}^{18}R$  is linked to the  $\delta^{18}O$  value through:

343

$$344 \quad \delta^{18}O = \left( \frac{{}^{18}R_{sample}}{{}^{18}R_{standard}} - 1 \right) \times 1000 \quad (4)$$

345

346 The isotopic discrimination is related to the isotopic fractionation factor through:

$$347 \quad {}^{18}\epsilon = {}^{18}\alpha - 1 \quad (5)$$

348 The same equations (3), (4) and (5) can be proposed for  $\delta^{17}O$  and the relationship between the  
349 fractionation factors  ${}^{17}\alpha$  and  ${}^{18}\alpha$  is written as:

$$350 \quad \theta = \frac{\ln {}^{17}\alpha}{\ln {}^{18}\alpha} \quad (6)$$

351

#### 352 **2.4.1. Soil respiration**

353 Respiration is associated with isotopic fractionation. The light isotopes,  ${}^{16}O$ , are more easily integrated  
354 by microorganisms than the heavy isotopes,  ${}^{18}O$ , which hence remain in the atmosphere. We express  
355 the fractionation factor for soil respiration as:

356

$$357 \quad {}^{18}\alpha_{soil\_respi} = \frac{{}^{18}R_{respired}}{{}^{18}R_{air}} \quad (7)$$

358

359 In our experiment, the respiratory process took place in a closed reservoir so that we could calculate  
360 the fractionation factors from the evolution of the concentration and isotopic composition of dioxygen  
361 in the chamber. The number of molecules of dioxygen in the air of the closed chamber,  $n(O_2)$ ,  
362 between time  $t$  and time  $t+dt$  can be written as:

363

$$364 \quad n(O_2)_{t+dt} = n(O_2)_t + dn(O_2) \quad (8)$$

365

366

367 with  $dn(O_2)$  the number of dioxygen molecules respired during the time period  $dt$ . A similar equation  
 368 can be written for the number of dioxygen molecules containing  $^{18}O$  remaining in the air of the  
 369 chamber:

370

$$371 \quad {}^{18}R_{t+dt} \times n(O_2)_{t+dt} = {}^{18}R_t \times n(O_2)_t + {}^{18}R_t \times {}^{18}\alpha_{soil\_respi} \times dn(O_2) \quad (9)$$

372

373 The evolution of the isotopic ratio of oxygen,  $^{18}R$ , between time  $t$  and time  $t+dt$  can be written as:

374

$$375 \quad {}^{18}R_{t+dt} = {}^{18}R_t + d^{18}R \quad (10)$$

376

377 Combining equations Eq. (8), (9) and (10), neglecting the second order term  $d^{18}R_t \times dn(O_2)_t$  and  
 378 integrating from  $t_0$  (starting time of the experiment when the chamber is closed) to  $t$  leads to:

379

$$380 \quad {}^{18}\epsilon_{soil\_respi} = {}^{18}\alpha_{soil\_respi} - 1 = \frac{\ln\left(\frac{\frac{\delta^{18}O_t+1}{1000}}{\frac{\delta^{18}O_{t_0}+1}{1000}}\right)}{\ln\left(\frac{n(O_2)_t}{n(O_2)_{t_0}}\right)} \quad (11)$$

381

382 Because argon is an inert gas, we can link  $\frac{n(O_2)_t}{n(O_2)_{t_0}}$  to  $\delta\left(\frac{O_2}{Ar}\right)$ , so that:

383

$$384 \quad \frac{n(O_2)_t}{n(O_2)_{t_0}} = \frac{\frac{\delta\left(\frac{O_2}{Ar}\right)_t+1}{1000}}{\frac{\delta\left(\frac{O_2}{Ar}\right)_{t_0}+1}{1000}} \quad (12)$$

385

386

### 387 2.4.2. Dark respiration

388 In order to calculate the isotopic fractionation associated with soil and plant respiration during dark  
 389 period, we followed the same calculation as for the soil respiration (section 2.4.1). In this case, we  
 390 selected only night periods from each sequence of the photosynthesis and dark respiration  
 391 experiment.

392

### 393 2.4.3. Photosynthesis

394 During photosynthesis, the oxygen atoms in the dioxygen produced by the plant comes from the  
395 oxygen atom of water consumed by photosynthesis in the leaves so that the fractionation factor during  
396 photosynthesis can be expressed as:

397

$$398 \quad {}^{18}\alpha_{photosynthesis} = \frac{{}^{18}R_{produced\ O_2}}{{}^{18}R_{lw}} \quad (13)$$

399

400 where *lw* stands for leaf water.

401 For our study of *Festuca arundinacea* we consider that the water in the mesophyll layer can be  
402 represented by bulk leaf water.

403

404 Photosynthesis occurs during the light periods. However, it should be noted that dark respiration,  
405 photorespiration and Mehler reaction occur at the same time. In a first approach, we did the  
406 assumption that respiration rates remain the same during the light and dark periods. This  
407 assumption is probably true for soil respiration since flux of heterotrophic dark respiration is not  
408 expected to change for different light conditions if the other environmental drivers (e.g. humidity,  
409 temperature, soil organic matter) are constant. However, autotrophic dark respiration is expected to  
410 decrease during light periods compared to dark periods. As a consequence, we present sensitivity  
411 tests to the dependence of a vanishing dark respiration of leaves during the dark period in Table S4.

412

413 Thus, at each stage, dioxygen is both produced by photosynthesis and consumed by the  
414 aforementioned  $O_2$  uptake processes (hereafter *total\_respi*) by the plant according to the mass  
415 conservation equation:

416

$$417 \quad n(O_2)_{t+dt} = n(O_2)_t + dn_{total\_respi} + dn_{photosynthesis} \quad (14)$$

418

419 where  $dn_{total\_respi}$  is the number of molecules of  $O_2$  consumed by dark respiration, photorespiration  
420 and Mehler reaction between time  $t$  and  $t+dt$ , and  $dn_{photosynthesis}$  is the number of molecules of  $O_2$   
421 produced by photosynthesis between  $t$  and  $t+dt$ .

422

423 The budget for  $^{18}O$  of  $O_2$  can be written as:

424

$$\begin{aligned}
425 \quad & {}^{18}R_{t+dt} \times \frac{n(O_2)_{t+dt}}{n(O_2)_{t0}} = {}^{18}R_t \times \frac{n(O_2)_t}{n(O_2)_{t0}} + {}^{18}R_t \times {}^{18}\alpha_{total\_respi} \times \frac{dn_{total\_respi}}{n(O_2)_{t0}} + {}^{18}R_{lw} \times \\
426 \quad & {}^{18}\alpha_{photosynthesis} \times \frac{dn_{photosynthesis}}{n(O_2)_{t0}} \quad (15)
\end{aligned}$$

427  
428 where  ${}^{18}\alpha_{total\_respi}$  is the fractionation factors associated with each  $O_2$  consuming process periods  
429 throughout the whole experiment.

430 We introduced the normalized fluxes of photosynthesis and total respiration as:

$$431 \\
432 \quad F_{photosynthesis} = \frac{dn_{photosynthesis}}{n(O_2)_{t0} \times dt} \quad (16)$$

$$433 \\
434 \quad F_{total\_respi} = \frac{dn_{total\_respi}}{n(O_2)_{t0} \times dt} \quad (17)$$

$$435 \\
436 \quad a^{18}R = \frac{d^{18}R}{dt} \quad (18)$$

437  
438 This led to the following expression of  ${}^{18}\alpha_{photosynthesis}$  :

$$\begin{aligned}
439 \\
440 \quad & {}^{18}\alpha_{photosynthesis} = \frac{n(O_2)_t / n(O_2)_{t0} \times a^{18}R + {}^{18}R_t \times (F_{photosynthesis} + F_{total\_respi} - {}^{18}\alpha_{total\_respi} \times F_{total\_respi})}{{}^{18}R_{lw} \times F_{photosynthesis}} \\
441 \\
442 \\
443 \quad & \quad (19)
\end{aligned}$$

444 This equation can be simplified at  $t=0$  for  ${}^{18}R_t = {}^{18}R_{t0} = 1$  and  $n(O_2)_t = n(O_2)_{t0}$ :

445  ${}^{18}\alpha_{photosynthesis}$  depends on the values of  ${}^{18}\alpha_{total\_respi}$  and of  $F_{total\_respi}$ , themselves dependent  
446 on the values of  ${}^{18}\alpha_{Mehler}$  (fractionation factor associated with Mehler reaction),  $F_{Mehler}$  (flux of  
447 oxygen related to Mehler reaction),  ${}^{18}\alpha_{dark\_respi}$ ,  $F_{dark\_respi}$ ,  ${}^{18}\alpha_{photorespi}$  (fractionation factor  
448 associated with photorespiration) and  $F_{photorespi}$  (photorespiration flux of oxygen). These last 4  
449 parameters could not be determined in our global experiment. Our determination of  ${}^{18}\alpha_{photosynthesis}$   
450 will thus rely on assumptions for the estimations of  ${}^{18}\alpha_{Mehler}$ ,  $F_{Mehler}$ ,  ${}^{18}\alpha_{photorespi}$  and  $F_{photorespi}$ .

451  
452 To separate the  ${}^{18}\alpha_{dark\_respi}$  from the other fractionation factors, we defined:

$$\begin{aligned}
453 \\
454 \quad & {}^{18}\alpha_{total\_respi} = {}^{18}\alpha_{photorespi} \times f_{photorespi} + {}^{18}\alpha_{Mehler} \times f_{Mehler} + {}^{18}\alpha_{dark\_respi} \times f_{dark\_respi} \\
455 \quad & \quad (20)
\end{aligned}$$

456 with

457

$$458 \quad F_{total\_respi} = F_{dark\_respi} + F_{photorespi} + F_{Mehler} \quad (21)$$

459

460

461  $f$  indicates the fraction of the total oxygen uptake flux corresponding to each process (dark  
462 respiration, photorespiration and Mehler reaction) so that:

463

$$464 \quad f_{dark\_respi} + f_{photorespi} + f_{Mehler} = 1 \quad (22)$$

465

$$466 \quad F_{dark\_respi} = f_{dark\_respi} \times F_{total\_respi} \quad (23)$$

467

$$468 \quad F_{photorespi} = f_{photorespi} \times F_{total\_respi} \quad (24)$$

469

$$470 \quad F_{Mehler} = f_{Mehler} \times F_{total\_respi} \quad (25)$$

471

472 In the absence of further constraints, we used here as first approximation the global values from  
473 Landais et al. (2007) for  $f_{dark\_respi}$  (0.6),  $f_{photorespi}$  (0.3) and  $f_{Mehler}$  (0.1). Values for  $\alpha_{photorespi}$  and  
474  $\alpha_{Mehler}$  were based on the most recent estimates of Helman et al. (2005).

475

476 **Table 1. List of variables used to quantify fractionations and their definitions.** \* means either oxygen  
477 17 or oxygen 18.

| Symbol                         | Definition  | Origin of the value             |
|--------------------------------|---|---------------------------------|
| * $\alpha$                     | Fractionation factor  |                                 |
| * $\alpha_{dark\_respi}$       | Fractionation factor of soil and plant respiration during night periods | Determined by our study         |
| * $\alpha_{dark\_leaf\_respi}$ | Fractionation factor of leaf respiration during night periods           | Determined by our study         |
| * $\alpha_{Mehler}$            | Fractionation factor associated with Mehler respiration                 | Value from Helman et al. (2005) |
| * $\alpha_{photorespi}$        | Fractionation factor associated with photorespiration                   | Value from Helman et al. (2005) |



|                                  |   |                         |
|----------------------------------|---|-------------------------|
| $^*\alpha_{photosynthesis}$      | Fractionation factor associated with photosynthesis   | Determined by our study |
| $^*\alpha_{soil\_respi}$         | Fractionation factor associated with soil respiration   | Determined by our study |
| $^*\alpha_{total\_respi}$        | Fractionation factor associated with total respiration during light period                          | Determined by our study |
| $^*\epsilon$                     | Isotopic discrimination   |                         |
| $^*\epsilon_{dark\_respi}$       | Isotopic discrimination of soil and plant respiration during night periods                          | Determined by our study |
| $^*\epsilon_{dark\_leaf\_respi}$ | Isotopic discrimination of leaf respiration during night periods                                    | Determined by our study |
| $^*\epsilon_{photosynthesis}$    | Isotopic discrimination associated with photosynthesis  | Determined by our study |
| $^*\epsilon_{soil\_respi}$       | Isotopic discrimination of soil respiration associated with soil respiration experiment             | Determined by our study |
| $\theta$                         | Ratio of $\ln(^{17}\alpha)$ to $\ln(^{18}\alpha)$   |                         |
| $\theta_{dark\_respi}$           | Ratio of $\ln(^{17}\alpha_{dark\_respi})$ to $\ln(^{18}\alpha_{dark\_respi})$                       | Determined by our study |
| $\theta_{dark\_leaf\_respi}$     | Ratio of $\ln(^{17}\alpha_{dark\_leaf\_respi})$ to $\ln(^{18}\alpha_{dark\_leaf\_respi})$           | Determined by our study |
| $\theta_{photosynthesis}$        | Ratio of $\ln(^{17}\alpha_{photosynthesis})$ to $\ln(^{18}\alpha_{photosynthesis})$                 | Determined by our study |
| $\theta_{soil\_respi}$           | Ratio of $\ln(^{17}\alpha_{soil\_respi})$ to $\ln(^{18}\alpha_{soil\_respi})$                       | Determined by our study |
| $aN$                             | Linear regression coefficient of the evolution of $n(O_2)$ as a function of time                    | Determined by our study |
| $a^*R$                           | Linear regression coefficient of the evolution of $R^*O$ as a function of time                      | Determined by our study |
| $dn_{photosynthesis}$            | Number of moles of $O_2$ produced by photosynthesis between t and t+dt                              | Determined by our study |
| $dn_{total\_respi}$              | Number of moles of $O_2$ consumed by total respiration during light periods between time t and t+dt | Determined by our study |
| $F_{dark\_respi}$                | Dark respiration flux (normalized vs number of moles of $O_2$ at the start of the experiment)       | Determined by our study |

|                      |  |   |
|----------------------|--|---|
| $F_{Mehler}$         | Mehler flux (normalized vs number of moles of O <sub>2</sub> at the start of the experiment)   | Determined by our study and Landais et al. (2007) |
| $F_{photorespi}$     | Photorespiration O <sub>2</sub> flux (normalized vs number of moles of O <sub>2</sub> at the start of the experiment)                      | Determined by our study and Landais et al. (2007) |
| $F_{photosynthesis}$ | Photosynthesis O <sub>2</sub> flux (normalized vs number of moles of O <sub>2</sub> at the start of the experiment)                        | Determined by our study                           |
| $F_{total\_respi}$   | Total respiration O <sub>2</sub> flux during light period (normalized vs number of moles of O <sub>2</sub> at the start of the experiment) | Determined by our study                           |
| $f_{dark\_respi}$    | Fraction of the dioxygen flux corresponding to dark respiration process  | Value from Landais et al. (2007)                  |
| $f_{Mehler}$         | Fraction of the dioxygen flux corresponding to Mehler process  | Value from Landais et al. (2007)                  |
| $f_{photorespi}$     | Fraction of the dioxygen flux corresponding to photorespiration process  | Value from Landais et al. (2007)                  |
| $n(O_2)$             | Number of moles of O <sub>2</sub>  | Determined by our study                           |
| $^*R$                | Ratio of heavy ( <sup>18</sup> O or <sup>17</sup> O) isotope to light isotope ( <sup>16</sup> O) of O <sub>2</sub> in air                  | Determined by our study                           |
| $^*R_{lw}$           | $^*R$ of leaf water  | Determined by our study                           |

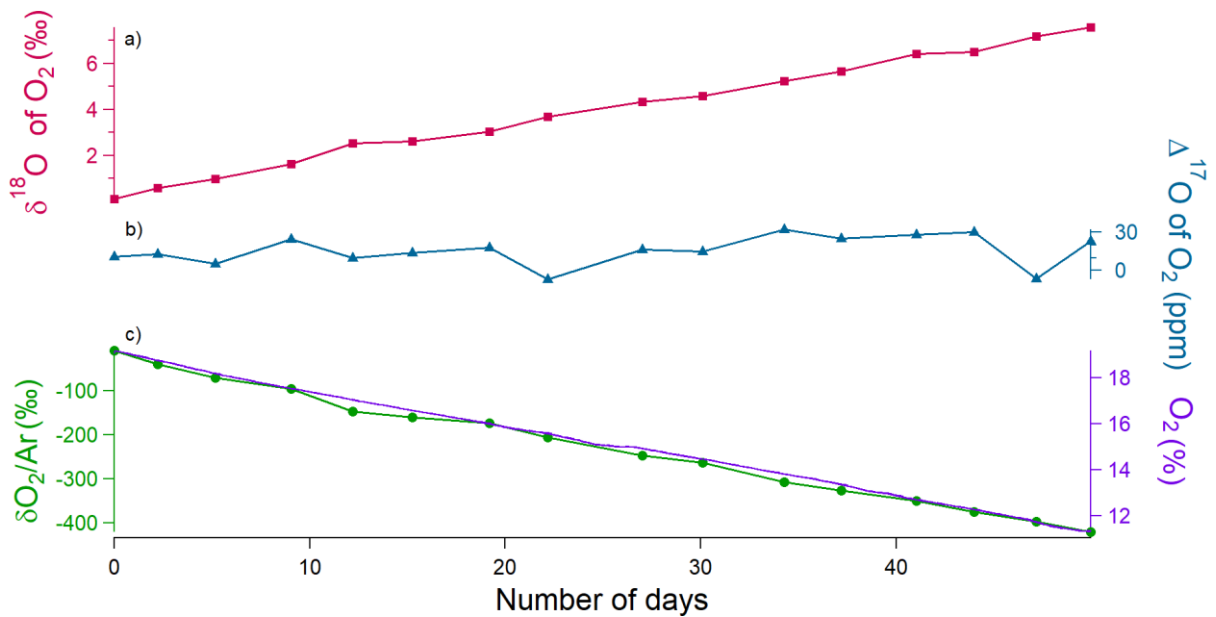
478

## 479 3.Results

### 480 3.1. Soil Respiration

#### 481 3.1.1. Experimental data

482



483

484

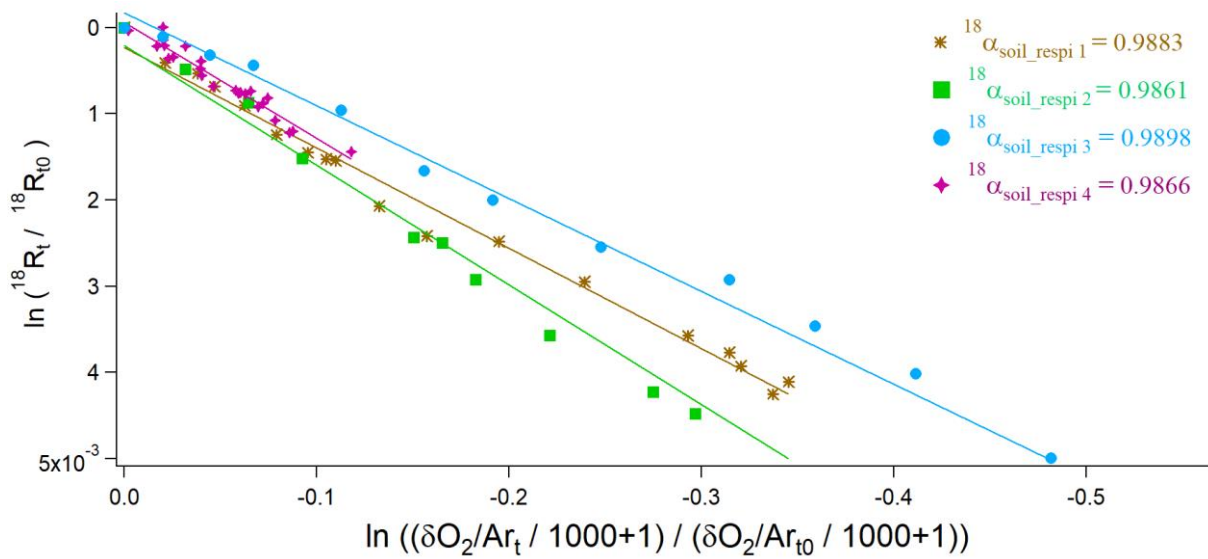
485 **Fig.2. Evolution of the different concentrations and isotopic ratios in the sequence 2 of the soil**  
486 **respiration experiment (day 0 is the beginning of the sequence). (a)  $\delta^{18}\text{O}$  of  $\text{O}_2$  (red) variations. (b)**  
487  **$\Delta^{17}\text{O}$  of  $\text{O}_2$  (blue) variations. (c) Dioxygen concentration (purple) from the optical sensor and  $\delta\text{O}_2/\text{Ar}$**   
488 **variations (green) measured by IRMS.**

489 During the 4 sequences, the respiration activity led to a decreasing level of the  $\text{O}_2$  concentration  
490 measured by the optical sensor or through the  $\delta\text{O}_2/\text{Ar}$  evolution from IRMS measurements (Fig. S1).  
491 The comparison of the evolution of the  $\text{O}_2$  concentration during the different sequences showed that  
492 respiratory fluxes were different with a maximum factor of 4 between the different sequences (Fig.  
493 S1). In parallel to the decrease in  $\text{O}_2$  concentration, the  $\delta^{18}\text{O}$  increased as expected because respiration  
494 preferentially consumes the lightest isotopes: over the 51 days of the 2<sup>nd</sup> soil respiration sequence, we  
495 observed a linear decrease of oxygen concentration by more than 5 % while  $\delta^{18}\text{O}$  increased by 8 ‰  
496 (Fig. 2). A Mann-Kendall trend test showed that the  $\Delta^{17}\text{O}$  of  $\text{O}_2$  does not show any statistically  
497 significant trend over the 4 sequences (Fig. S2) (p-values were equal to 0.40, 0.08, 0.58, 0.47,  
498 respectively).

### 499 **3.1.2. Fractionation factors**

500 We used the 15 to 20 samples obtained during each sequence of soil respiration experiment to draw  
501 the relative evolution of  $\ln(^{18}\text{R}_t/^{18}\text{R}_{t0})$  vs  $\ln((\delta(\frac{\text{O}_2}{\text{Ar}})_t/1000 + 1)/(\delta(\frac{\text{O}_2}{\text{Ar}})_{t0}/1000 + 1))$   
502 following Eq. (11) (Fig. 3). The slope of the corresponding regression line provided the isotopic  
503 discrimination  $^{18}\epsilon_{\text{soil\_respi}}$  and hence the fractionation factor  $^{18}\alpha_{\text{soil\_respi}}$  for each sequence (Table  
504 S5). It could be observed that despite differences in respiratory fluxes for the different sequences (the  
505 standard deviation is equal to 50 % of the average flux across sequences; see Table S5), the relationship  
506 between  $\delta^{18}\text{O}$  of  $\text{O}_2$  and  $\text{O}_2$  concentration (or  $\delta\text{O}_2/\text{Ar}$ ), and hence the calculated fractionation factor  
507 associated with respiration, is not much affected.

508



509

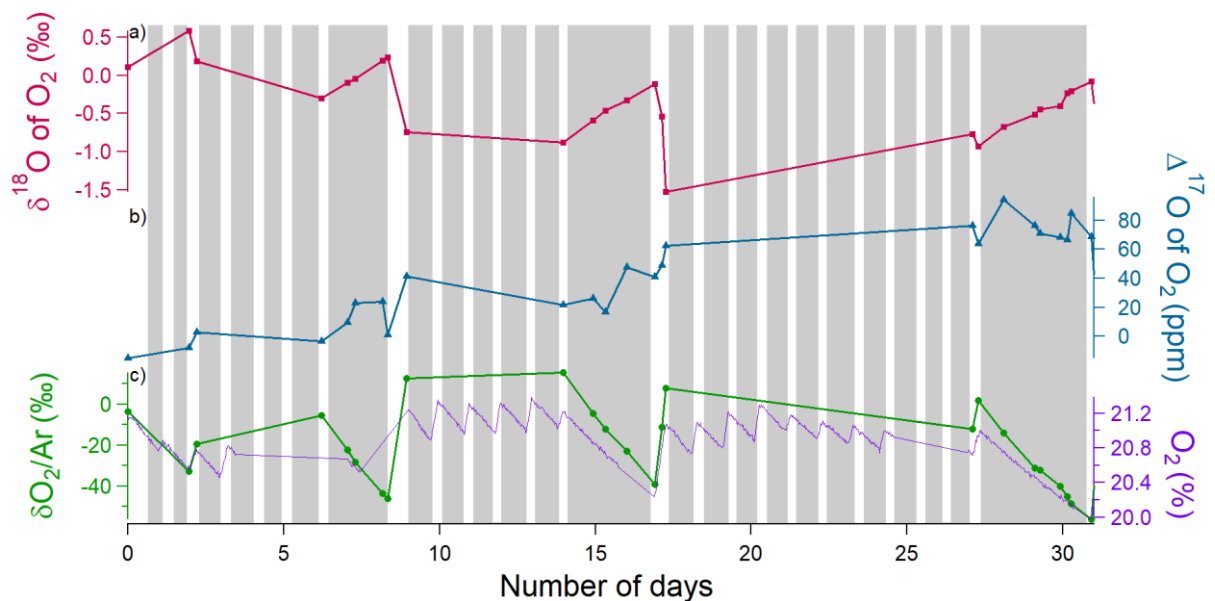
510 **Fig.3 Determination of  $^{18}\text{O}/^{16}\text{O}$  fractionation factors in the 4 respiration sequences.**  
 511  $^{18}\alpha_{soil\_respi\ 1}$  (brown),  $^{18}\alpha_{soil\_respi\ 2}$  (green),  $^{18}\alpha_{soil\_respi\ 3}$  (blue),  $^{18}\alpha_{soil\_respi\ 4}$  (purple) are  
 512 respectively respiratory fractionation factors associated with sequences 1 to 4.

513 Using the results of the 4 sequences, we determined the values for the mean isotopic discrimination  
 514  $^{18}\epsilon_{soil\_respi}$  ( $-12.3 \pm 1.7$  ‰), the mean isotopic discrimination  $^{17}\epsilon_{soil\_respi}$  ( $-6.4 \pm 0.9$  ‰) and the  
 515 average  $\theta_{soil\_respi}$  ( $0.5164 \pm 0.0005$ ).

516

### 517 3.2. Photosynthesis and dark respiration

#### 518 3.2.1. Experimental data



519

520 **Fig.4. Example of the evolution of the different concentrations and isotopic ratios in the sequence 1**  
 521 **of photosynthesis and dark respiration experiment in the closed chamber over 31 days (day 0 is the**  
 522 **beginning of the sequence). Grey rectangles correspond to night periods and white rectangles to**  
 523 **light periods. (a)  $\delta^{18}\text{O}$  of  $\text{O}_2$  (red) variations. (b)  $\Delta^{17}\text{O}$  of  $\text{O}_2$  variations (blue). (c) Dioxygen**  
 524 **concentration (purple) from the optical sensor and  $\delta\text{O}_2/\text{Ar}$  variations (green) measured by IRMS.**

525  
 526 During the night periods, when only respiration occurred, we observed a decrease in  $\text{O}_2$  concentration  
 527 by 1% within 3 days and a  $\delta^{18}\text{O}$  increase by 1‰ during the same period (Fig. 4). The evolution was  
 528 qualitatively similar with that of soil respiration experiments with higher fluxes. We observed the same  
 529 trends for the evolution of  $\delta\text{O}_2/\text{Ar}$  during the night periods as for the respiration experiment. During  
 530 light periods, there was a marked decrease in  $\delta^{18}\text{O}$  (2 ‰) and a marked increase in the flux of oxygen  
 531 released (1%) during 1 day. We observed the same trends for the evolution of  $\delta\text{O}_2/\text{Ar}$  during the night  
 532 periods as for the respiration experiment.

533  
 534 The Mann-Kendall test (95%) showed a significative increasing trend of the  $\Delta^{17}\text{O}$  of  $\text{O}_2$  over sequences  
 535 1 and 2 (Fig. S3) ( $\approx 100$  ppm in 31 days for sequence 1,  $\approx 100$  ppm in 40 days for sequence 2) while  
 536 no significant increase of  $\Delta^{17}\text{O}$  of  $\text{O}_2$  is observed over sequence 3 (Fig. S3).

537

### 538 **3.2.2. Fractionation factors**

#### 539 **Dark respiration**

540 The average of the isotopic discrimination for dark respiration  $^{18}\epsilon_{\text{dark\_respi}}$  and  $^{17}\epsilon_{\text{dark\_respi}}$  were  
 541 calculated over the 9 night periods and we obtained values of respectively  $-17.0 \pm 2.0$  ‰ and  $-8.5 \pm$   
 542  $0.8$  ‰. The average of  $\theta_{\text{dark\_respi}}$  during the experiment was equal to  $0.5124 \pm 0.0084$  (details in Table  
 543 S6).

544 The dark respiration of this experiment includes respiration of both soil and leaves. Because soil  
 545 respiration fractionation factor has been determined above, it is possible to estimate here the  
 546 fractionation factor for the dark leaf respiration and we consider that respiration rate during dark and  
 547 light periods do not vary:

548

$$549 \quad F_{\text{dark\_respi}} = F_{\text{soil\_respi}} + F_{\text{dark\_leaf\_respi}} \quad (26)$$

$$550 \quad ^{18}\alpha_{\text{dark\_respi}} = f_{\text{soil\_respi}} \times ^{18}\alpha_{\text{soil\_respi}} + f_{\text{dark\_leaf\_respi}} \times ^{18}\alpha_{\text{dark\_leaf\_respi}} \quad (27)$$

551

552 with  $F_{dark\_leaf\_respi}$  the flux of leaf respiration during the night,  $f_{soil\_respi}$  the fraction of soil  
 553 respiration during night periods ( $F_{soil\_respi} / F_{dark\_respi}$ ) and  $f_{dark\_leaf\_respi}$  the fraction of dark leaf  
 554 respiration during night periods ( $F_{dark\_leaf\_respi} / F_{dark\_respi}$ ).

555

$$556 \quad {}^{18}\alpha_{dark\_leaf\_respi} = \frac{{}^{18}\alpha_{dark\_respi} - f_{soil\_respi} \times {}^{18}\alpha_{soil\_respi}}{f_{dark\_leaf\_respi}} \quad (28)$$

557

558 The isotopic discriminations  ${}^{18}\epsilon_{dark\_leaf\_respi}$  and  ${}^{17}\epsilon_{dark\_leaf\_respi}$  were respectively equals to  $-19.1$   
 559  $\pm 2.4$  ‰ and  $-9.7 \pm 0.9$  ‰. The average of  $\theta_{dark\_leaf\_respi}$  was equal to  $0.5089 \pm 0.0777$ . The standard  
 560 deviations ( $1\sigma$ ) was calculated by a Monte Carlo method from the individual uncertainties of the  
 561  ${}^{18}\alpha_{dark\_respi}$ ,  ${}^{18}\alpha_{soil\_respi}$ ,  $F_{soil\_respi}$  and  $F_{dark\_respi}$ .

562

### 563 **Photosynthesis**

564 In order to calculate an average value for the fractionation factor associated with photosynthesis from  
 565 Eq. (19), we first calculated the averages of the flux of the  $O_2$  consuming processes and of the  
 566 fractionation factors associated with each sequence:  $\langle F_{total\_respi} \rangle$  and  $\langle {}^{18}\alpha_{total\_respi} \rangle$ . We also  
 567 calculated the net  $O_2$  flux during light periods,  $aN = F_{photosynthesis} + F_{total\_respi}$ , as the linear  
 568 regression,  $aN$ , of  $\frac{n(O_2)_t}{n(O_2)_{t0}}$  with time.  $a^{18}R$  is also obtained as a linear regression of  ${}^{18}R$  with time over  
 569 each light period. Our data support our assumption that the regime was stationary over time and  
 570  $n(O_2)_t / n(O_2)_{t0}$  evolved linearly over time, which is why we were able to do linear regressions.

571

$$572 \quad {}^{18}\alpha_{photosynthesis} = \frac{a^{18}R + aN - \langle {}^{18}\alpha_{total\_respi} \rangle \times \langle F_{total\_respi} \rangle}{{}^{18}R_{lw} \times F_{photosynthesis}} \quad (29)$$

573

574

575 The results of the 8 individuals  $\alpha_{photosynthesis}$  values are given in Table S10. The value of isotopic  
 576 fractionation associated with the light period of period 1 of sequence 1 appeared clearly out of range.  
 577 Following the Dixon's outlier detection test (Dixon, 1960), this value was considered an anomaly  
 578 (likelihood > 99 %) and was removed from further analysis.

579

580 We finally estimated the values of  ${}^{18}\epsilon_{photosynthesis}$  and  ${}^{17}\epsilon_{photosynthesis}$  as  $+3.7 \pm 1.3$  ‰ and  $+1.9$   
 581  $\pm 0.6$  ‰, respectively. The average of  $\theta_{photosynthesis}$  was equal to  $0.5207 \pm 0.0537$ , a value which

582 depends on the value taken for the  $\delta^{17}\text{O}$  value of atmospheric  $\text{O}_2$  vs VSMOW (Sharp and Wostbrock,  
583 2021), see Table 2.

584 We performed different sensitivity tests (supplementary texts 1 and 2). Sensitivity test 1 (Table S4)  
585 quantifies the influence of vanishing flux of dark leaf respiration during the day. This test shows that  
586 the assumption of similar flux of dark leaf respiration during the night and light periods did not  
587 influence much the values of photosynthesis fractionation factors. It results in an additional  
588 uncertainty of 0.0006 and 0.0005 for the values of  $^{18}\alpha_{\text{photosynthesis}}$  and  $^{17}\alpha_{\text{photosynthesis}}$ .

589 Sensitivity tests 2 (Tables S7, S8 and S9) were performed on values of the  $\text{O}_2$  flux and associated  
590 fractionation factors for photorespiration and Mehler reaction. They resulted in additional  
591 uncertainties of 0.0007 and 0.0005 for the values of  $^{18}\alpha_{\text{photosynthesis}}$  and  $^{17}\alpha_{\text{photosynthesis}}$  (Table  
592 S10).

593 Sensitivity tests 3 concerned the possible evolution of the isotopic composition of leaf water on the  
594 course of an experiment. The comparison of the  $\delta^{18}\text{O}$  of irrigation water and soil water at the end of  
595 the experiment shows a possible increase up to 2‰ (Table S3). We thus estimate that our values of  
596 leaf water  $\delta^{18}\text{O}$  measured at the end of the experiment may be overestimated by 1‰ compared to the  
597 mean value of leaf water  $\delta^{18}\text{O}$  during the course of the experiment. Taking this possible effect into  
598 account would lead to a fractionation factor for photosynthesis higher by 1‰ compared to the  
599 presented one of  $3.7 \pm 1.3$  ‰, hence a higher isotopic discrimination associated with photosynthesis.

600

## 601 4. Discussion

### 602 4.1. $\Delta^{17}\text{O}$ of $\text{O}_2$

603 The  $\Delta^{17}\text{O}$  of  $\text{O}_2$  is equal to 0 by definition for atmospheric air, and hence it should be equal to zero at  
604 the beginning of each experiment. The observed change during an experiment can only be driven by  
605 biological processes because the interaction with stratosphere is not possible in the closed chambers.

606 During the soil respiration experimental run, the  $\Delta^{17}\text{O}$  of  $\text{O}_2$  was constant. This directly reflects the  
607  $\theta_{\text{soil\_respi}}$  value of  $0.5164 \pm 0.0005$  found for respiration (Table 2) because  $\Delta^{17}\text{O}$  of  $\text{O}_2$  is defined with  
608 a slope of 0.516 between  $\ln(1 + \delta^{17}\text{O})$  and  $\ln(1 + \delta^{18}\text{O})$  (Eq. 1). This result is in good agreement and  
609 within the uncertainties given by Helman et al. (2005) with the  $\gamma$  value of  $0.5174 \pm 0.0003$  obtained  
610 with respiration experiments on several micro-organisms.

611 During the experiment involving both oxygen uptake and photosynthesis, the  $\Delta^{17}\text{O}$  of  $\text{O}_2$  has a globally  
612 increasing trend with values reaching about 100 ppm after one month. Such behavior is expected and

613 was already observed by Luz et al. (1999) with  $\Delta^{17}\text{O}$  of  $\text{O}_2$  values reaching 150 ppm after a 200-day  
614 experiment within a closed terrarium. This increase cannot be explained by respiration because  
615 respiration does not modify  $\Delta^{17}\text{O}$  of  $\text{O}_2$ . It is hence mainly due to photosynthesis producing oxygen  
616 with a  $\Delta^{17}\text{O}$  of  $\text{O}_2$  different from the atmospheric one. Previous analyses have shown that the  $\Delta^{17}\text{O}$  of  
617  $\text{H}_2\text{O}$  of VSMOW (close to mean oceanic water) expressed vs isotopic composition of atmospheric  $\text{O}_2$   
618 has a value between 134 to 223 ppm (using a definition of  $\Delta^{17}\text{O}$  of  $\text{H}_2\text{O} = \ln(1+\delta^{17}\text{O}) - 0.516 \times \ln(1+\delta^{18}\text{O})$ )  
619 (Sharp and Wostbrock, 2021). Within the water cycle, the slopes of  $\ln(1+\delta^{17}\text{O})$  vs  $\ln(1+\delta^{18}\text{O})$  for the  
620 meteoric line, evaporation and evapotranspiration lines are larger than 0.516 (Li and Meijer, 1998;  
621 Landais et al., 2006) so that  $\Delta^{17}\text{O}$  of water consumed by the plants during photosynthesis should be  
622 slightly lower than the  $\Delta^{17}\text{O}$  of VSMOW expressed vs isotopic composition of atmospheric  $\text{O}_2$  but still  
623 higher than the  $\Delta^{17}\text{O}$  of atmospheric  $\text{O}_2$ . The photosynthesis is thus responsible for the  $\Delta^{17}\text{O}$  of  $\text{O}_2$   
624 increase in the closed chamber.

625

#### 626 4.2. Fractionation factors associated with $\delta^{18}\text{O}$ of $\text{O}_2$ and implications for the Dole effect

627 **Table 2. Summary of the mean values of the isotopic discriminations and gamma values for *Festuca***  
628 ***arundinacea* of all sequences of (1) the soil respiration experiment and of (2) the respiration and**  
629 **photosynthesis experiment and the number of data on which they were calculated. \*\* is the value**  
630 **for  $\theta_{\text{photosynthesis}}$  that depends on the determination of the  $\delta^{17}\text{O}$  of atmospheric  $\text{O}_2$  vs  $\delta^{17}\text{O}$  of**  
631 **VSMOW. We provide here the two different possible estimates using either 12.03 ‰ (Luz and Barkan,**  
632 **2011) or 12.08 ‰ (Barkan and Luz, 2005): value determined with  $\delta^{17}\text{O} = 12.03$  ‰ / value determined**  
633 **with  $\delta^{17}\text{O} = 12.08$  ‰.**

634

| Isotopic discriminations and gamma values of <i>Festuca arundinacea</i> | Average (‰) | Standard deviation (‰) | Number of data |
|---|-------------|------------------------|----------------|
| $^{18}\epsilon_{\text{soil\_respi}}$                                    | -12.3       | 1.7                    | 4              |
| $^{17}\epsilon_{\text{soil\_respi}}$                                    | -6.4        | 0.9                    | 4              |
| $\theta_{\text{soil\_respi}}$   | 0.5164      | 0.0005                 | 4              |
| $^{18}\epsilon_{\text{dark\_respi}}$                                    | -17.0       | 2.0                    | 9              |
| $^{17}\epsilon_{\text{dark\_respi}}$                                    | -8.5        | 0.8                    | 9              |
| $\theta_{\text{dark\_respi}}$   | 0.5124      | 0.0084                 | 9              |
| $^{18}\alpha_{\text{dark\_leaf\_respi}}$                                | -19.1       | 2.4                    | 9              |



|                                   |                 |                 |   |
|-----------------------------------|-----------------|-----------------|---|
| $^{17}\alpha_{dark\_leaf\_respi}$ | -9.7            | 0.9             | 9 |
| $\theta_{dark\_leaf\_respi}$      | 0.5089          | 0.0777          | 9 |
| $^{18}\epsilon_{photosynthesis}$  | 3.7             | 1.3             | 8 |
| $^{17}\epsilon_{photosynthesis}$  | 1.9             | 0.6             | 8 |
| $\theta_{photosynthesis}$         | 0.5207/0.5051** | 0.0537/0.0504** | 8 |

635

636 The isotopic discrimination  $^{18}\epsilon_{soil\_respi} = -12.3 \pm 1.7 \text{ ‰}$  for the soil respiration experiments is  
637 comparable to the average terrestrial soil respiration isotopic discrimination found by Angert et al.  
638 (2001) of  $-12 \text{ ‰}$ . Still, among the diversity of soils studied by Angert et al. (2001), the soils showing  
639 the  $^{18}\epsilon$  values closest to our values are clay soil ( $^{18}\epsilon = -13 \text{ ‰}$ ) and sandy soil ( $^{18}\epsilon = -11 \text{ ‰}$ ). Soil  
640 respiration isotopic discriminations are less strong than isotopic discrimination due to dark respiration  
641 alone ( $-18 \text{ ‰}$ , Bender et al., 1994). These lower values for soil respiration isotopic discrimination are  
642 due to the roles of root diffusion in the soil (Angert and Luz, 2001). The soils studied by Angert and Luz  
643 (2001) are however different from our soil which was enriched in organic matter. Further experiments  
644 are then needed to understand the variability in  $^{18}\epsilon$  associated with soil respiration.

645 The isotopic discrimination for dark leaf respiration,  $^{18}\epsilon_{dark\_leaf\_respi} = -19.1 \pm 2.4 \text{ ‰}$  is associated  
646 with a large uncertainty and would benefit from additional experiments with a higher sampling and  
647 measurement rate. Still, even if it was obtained on different organism and experimental set-up, this  
648 value is in agreement with the values for isotopic discrimination for dark respiration determined by  
649 Helman et al. (2005) on bacteria from the Lake Kinneret ( $^{18}\epsilon = -17.1 \text{ ‰}$ ) and *Synechocystis* ( $^{18}\epsilon = -19.4$   
650  $\text{ ‰}$  and  $-19.5 \text{ ‰}$ ).

651 The average  $^{18}\epsilon_{photosynthesis}$  is  $+3.7 \pm 1.3 \text{ ‰}$  for *Festuca arundinacea* species which goes against the  
652 classical assumption that terrestrial photosynthesis does not fractionate (Vinogradov et al., 1959; Guy  
653 et al., 1993; Helman et al., 2005; Luz & Barkan, 2005). Vinogradov explains that the low photosynthetic  
654 isotopic discrimination that can occur is due to contamination by atmospheric  $O_2$  or by respiration.  
655 Guy et al. (1993) corroborate this idea by finding a photosynthetic isotopic discrimination of  $0.3 \text{ ‰}$  in  
656 cyanobacteria (*Anacystis nidulans*) and diatoms (*Phaeodactylum tricornutum*) that they consider  
657 negligible. Luz and Barkan (2005) in their study on *Philodendron*, consider that there is no  
658 photosynthetic isotopic discrimination. Our value proves that there is indeed a terrestrial  
659 photosynthetic isotopic discrimination and the value found for *Festuca arundinacea* is slightly smaller  
660 than the photosynthetic isotopic discrimination in marine environment  $^{18}\epsilon_{photosynthesis} = +6 \text{ ‰}$   
661 found by Eisenstadt et al. (2010). More specifically, Eisenstadt et al. (2010) determined several

662 photosynthetic isotopic discrimination values depending on the phytoplankton studied  
663 (*Phaeodactylum tricornutum* = 4.5 ‰, *Nannocloreopsis sp.* = 3 ‰, *Emiliana huxleyi* = 5.5 ‰ and  
664 *Chlamydomonas reinhardtii* = 7 ‰). One of the conclusions given by Eisenstadt et al. (2010) is that  
665 eukaryotic organisms enrich their produced oxygen more in <sup>18</sup>O than prokaryotic organisms. Our  
666 conclusion based on experiments performed with *Festuca arundinacea* species is in agreement with  
667 these conclusions. We should however note that we tested only one species. Additional experiments  
668 with different plants are needed to check if this fractionation factor should be applied for global Dole  
669 effect calculation. Still, this positive <sup>18</sup>O discriminations during photosynthesis suggests that the  
670 terrestrial Dole effect may be higher than currently assumed and challenge the assumption that  
671 terrestrial and oceanic Dole effects have the same values (Luz and Barkan, 2011).

672

#### 673 4-Conclusion

674 Using a simplified analog of the terrestrial biosphere in a closed chamber we found that the  
675 fractionation factors of soil respiration and dark leaf respiration at the biological chamber level agree  
676 with the previous estimates derived from studies at micro-organism level. This is an important  
677 confirmatory step for the fractionation factors previously used to estimate the global Dole effect. More  
678 importantly, we document for the first time a significant <sup>18</sup>O discrimination during terrestrial  
679 photosynthesis with the *Festuca arundinacea* species (+ 3.7 ‰ ± 1.3 ‰). If confirmed by future studies,  
680 this can have a substantial impact on the calculation of the Dole effect, with important consequences  
681 for our estimates of the past global primary production.

682 Our study showed the usefulness of closed chamber systems to quantify the fractionation factors  
683 associated with biological processes in the oxygen cycle at the plant level. The main limitation of our  
684 present study was the low sampling rate during our experiments which hamper the precision of the  
685 determined fractionation factors. Future work should use this validated set-up to multiply such  
686 experiments to improve the precision of fractionation factors and to explore the variability of  
687 fractionation factors for different plants and hence different metabolisms. A good application would  
688 be to study the difference between C3 and C4 plants because C4 plants do not photorespire. C4 plants,  
689 adapted to dry environments, have their own strategy and make very little photorespiration through  
690 specialized cells. This allows them to produce their own energy in an optimal way without the waste  
691 produced by photorespiration.

692

#### 693 Data availability

694 All individual fractionation factors for each experiment are given in the Supplement.

695

## 696 Author contributions

697 AL and CPi designed the project. CPi, JS and SD carried out experiments at ECOTRON of Montpellier  
698 and FP, CPa, RJ, AD and OJ at LSCE. CPa, NP and AL analyzed the data. CPa and AL prepared the  
699 manuscript with contributions from NP, CPi, JS and AM.

700

## 701 Competing interests

702 The authors declare that they have no conflict of interest.

703

## 704 Acknowledgements

705 The research leading to these results has received funding from the European Research Council under  
706 the European Union H2020 Programme (H2020/20192024)/ERC grant agreement no. 817493 (ERC  
707 ICORDA) and ANR HUM17. The authors acknowledge the scientific and technical support of PANOPLY  
708 (Plateforme ANalytique géOsciences Paris-saclaY), Paris-Saclay University, France. This study  
709 benefited from the CNRS resources allocated to the French ECOTRONS Research Infrastructure, from  
710 the Occitanie Region and FEDER investments as well as from the state allocation 'Investissement  
711 d'Avenir' AnaEE- France ANR-11-INBS-0001. We would also like to thank Abdelaziz Faez and Olivier  
712 Ravel from ECOTRON of Montpellier for their help, Anne Alexandre from CEREGE at Aix-en-Provence  
713 and Emeritus Prof. Phil Ineson from University of York.

714

## 715 References

716 Alexandre, A., Landais, A., Vallet-Coulomb, C., Piel, C., Devidal, S., Pauchet, S., Sonzogni, C., Couapel,  
717 M., Pasturel, M., Cornuault, P., Xin, J., Mazur, J-C., Prié, F., Bentaleb, I., Webb, E., Chalié, F., and Roy,  
718 J.: The triple oxygen isotope composition of phytoliths as a proxy of continental atmospheric  
719 humidity: insights from climate chamber and climate transect calibrations, *Biogeosciences*, 15,  
720 3223-3241, <https://doi.org/10.5194/bg-15-3223-2018>, 2018.

721

722 Angert, A., Luz, B., and Yakir, D.: Fractionation of oxygen isotopes by respiration and diffusion in

723 soils and its implications for the isotopic composition of atmospheric O<sub>2</sub>, *Global Biogeochem. Cy.*,  
724 15, 871-880, <https://doi.org/10.1029/2000GB001371>, 2001.

725

726 Angert, A., Barkan, E., Barnett, B., Brugnoli, E., Davidson, E. A., Fessenden, J., Maneepong, S.,  
727 Panapitukkul, N., Randerson, J. T., Savage, K., Yakir, D., and Luz, B.: Contribution of soil respiration in  
728 tropical, temperate, and boreal forests to the <sup>18</sup>O enrichment of atmospheric O<sub>2</sub>, *Global*  
729 *Biogeochem. Cy.*, 17, 1089, <https://doi.org/10.1029/2003GB002056>, 2003.

730

731 Barkan, E., and Luz, B.: High precision measurements of <sup>17</sup>O/<sup>16</sup>O and <sup>18</sup>O/<sup>16</sup>O of O<sub>2</sub> and O<sub>2</sub>/Ar ratio in  
732 air, *Rapid Commun. Mass Spectrom.*, 17, 2809-2814, <https://doi.org/10.1002/rcm.1267>, 2003.

733

734 Barkan, E., and Luz, B.: High precision measurements of <sup>17</sup>O/<sup>16</sup>O and <sup>18</sup>O/<sup>16</sup>O ratios in H<sub>2</sub>O, *Rapid*  
735 *Commun. Mass Spectrom.*, 19, 3737-3742, <https://doi.org/10.1002/rcm.2250>, 2005.

736

737 Bauwe, H., Hagemann, M., and Fernie, A.R.: Photorespiration: players, partners and origin, *Trends*  
*Plant Sci.*, 6, 330-336, <https://doi.org/10.1016/j.tplants.2010.03.006> , 2010.

738

739 Bender, M., Sowers, T., Dickson, M-L., Orchardo, J., Grootes, P., Mayewski, P. A., and Meese, D. A.:  
740 Climate correlations between Greenland and Antarctica during the past 100,000 years, *Nature*, 372,  
741 663-666, <https://doi.org/10.1038/372663a0>, 1994.

742

743 Blunier, T., Barnett, B., Bender, M. L., and Hendricks, M. B.: Biological oxygen productivity during the  
744 last 60,000 years from triple oxygen isotope measurements, *Global Biogeochem. Cy.*, 16, 3-4,  
745 <https://doi.org/10.1029/2001GB001460>, 2002.

746

747 Brandon, M., Landais, A., Duchamp-Alphonse, S., Favre, V., Schmitz, L., Abrial, H., Prié, F., Extier, T.,  
748 and Blunier, T.: Exceptionally high biosphere productivity at the beginning of Marine Isotopic Stage  
749 11, *Nat. Commun.*, 11, 1-10, <https://doi.org/10.1038/s41467-020-15739-2>, 2020.

750

751 Dansgaard, W.: Stable isotopes in precipitation, *Tellus*, 16, 436-468, 1974.

752

753 Davidson, E.A., Janssens, I.A., and Luo, Y.: On the variability of respiration in terrestrial ecosystems:  
754 moving beyond Q<sub>10</sub>, *Glob. Change Biol.*, 12, 154-164, [https://doi.org/10.1111/j.1365-](https://doi.org/10.1111/j.1365-2486.2005.01065.x)  
755 2486.2005.01065.x, 2005.

756 Dixon, W. J.: Simplified estimation from censored normal sample, *Ann. Math. Stat.*, 21, 488-506,  
757 <https://doi.org/10.1214%2Faoms%2F1177729747>, 1960.

758

759 Dole, M., Lane, G. A., Rudd, D. P., and Zaukelies, D. A.: Isotopic composition of atmospheric oxygen  
760 and nitrogen, *Geochim. Cosmochim. Ac.*, 6, 65-78, [https://doi.org/10.1016/0016-7037\(54\)90016-2](https://doi.org/10.1016/0016-7037(54)90016-2),  
761 1954.

762

763 Dongman, G., Nürnberg, H. W., Förstel, H., and Wagener, K.: On the enrichment of H<sub>2</sub><sup>18</sup>O in the  
764 leaves of transpiring plants, *Radiat Environ Biophys*, 11, 41-52,  
765 <https://doi.org/10.1007/BF01323099>, 1974.

766

767 Dreyfus, G. B., Parrenin, F., Lemieux-Dudon, B., Durand, G., Masson-Delmotte, V., Jouzel, J.,  
768 Barnola<sup>3</sup>, J-M., Panno<sup>5</sup>, L., Spahni, R., Tisserand, A., Siegenthaler, U., and Leuenberger, M.:  
769 Anomalous flow below 2700 m in the EPICA Dome C ice core detected using  $\delta^{18}\text{O}$  of atmospheric  
770 oxygen measurements, *Clim. Past*, 3, 341-353, <https://doi.org/10.5194/cp-3-341-2007>, 2007.

771

772 Eisenstadt, D., Barkan, E., Luz, B., and Kaplan, A.: Enrichment of oxygen heavy isotopes during  
773 photosynthesis in phytoplankton, *Photosynth. Res.*, 103, 97-103,  
774 <https://doi.org/10.1007/s11120-009-9518-z>, 2010.

775

776 Extier, T., Landais, A., Bréant, C., Prié, F., Bazin, L., Dreyfus, G., Roche, D. M., Leuenberger, M.: On  
777 the use of  $\delta^{18}\text{O}_{\text{atm}}$  for ice core dating, *Quat. Sci. Rev.*, 185, 244-257,  
778 <https://doi.org/10.1016/j.quascirev.2018.02.008>, 2018.

779

780 Guy, R. D., Fogel, M.L., and Berry, J. A.: Photosynthetic fractionation of the stable isotopes of oxygen  
781 and carbon, *Plant Physiol.*, 101, 37-47, <https://doi.org/10.1104/pp.101.1.37>, 1993.

782

783 Helman, Y., Barkan, E., Eisenstadt, D., Luz, B., and Kaplan, A.: Fractionation of the three stables  
784 oxygen isotopes by oxygen-producing and oxygen-consuming reactions in photosynthetic  
785 organisms, *Plant Physiol.*, 138, 2292-2298, <https://doi.org/10.1104/pp.105.063768>, 2005.

786

787 Hillaire-Marcel, C., Kim, S-T., Landais, A., Ghosh, P., Assonov., S., Lécuyer, C., Blanchard, M., Meijer,  
788 H. A. J., and Steen-Larsen, H.: A stable isotope toolbox for water and inorganic carbon cycle studies,  
789 *Nat. Rev. Earth Environ*, 2, 699-719, <https://doi.org/10.1038/s43017-021-00209-0> , 2021.

790

791 Hoffmann, G., Cuntz, M., Weber, C., Ciais, P., Friedlingstein, P., Heimann, M., Jouzel, J., Kaduk, J.,  
792 Maier Reimer, E., Seibt, U., and Six, K.: A model of the Earth's Dole effect, *Global Biogeochem. Cy.*,  
793 18, 1-15, <https://doi.org/10.1029/2003GB002059>, 2004.

794 Keenan, T.F., Migliavacca M., Papale, D., Baldocchi, D., Reichstein, M., Torn, M., and Wutzler, T.:  
795 Widespread inhibition of daytime ecosystem respiration, *Nat. Ecol. Evol.*, 3, 407-415,  
796 <https://doi.org/10.1038/s41559-019-0809-2>, 20194.

797

798 Landais, A., Barkan, E., Yakir, D., and Luz, B.: The triple isotopic composition of oxygen in leaf water,  
799 *Geochim. Cosmochim. Ac.*, 70, 4105-4115, <https://doi.org/10.1016/j.gca.2006.06.1545>, 2006.

800

801 Landais, A., Dreyfus, G., Capron, E., Masson-Delmotte, V., Sanchez-Goñi, M. F., Desprat, S.,  
802 Hoffmann, G., Jouzel, J., Leuenberger and M., Johnsen, S.: What drives the orbital and millennial  
803 variations of  $d^{18}O_{atm}$ ?, *Quat. Sci. Rev.*, 29, 235-246, <https://doi.org/10.1016/j.quascirev.2009.07.005>,  
804 2010.

805

806 Luz, B., and Barkan, E.: The isotopic composition of atmospheric oxygen, *Global Biogeochem. Cy.*,  
807 25, GB3001, <https://doi.org/10.1029/2010GB003883>, 2011.

808

809 Luz, B., Barkan, E., Bender, M. L., Thiemens, M. H., and Boering, K. A.: Triple-isotope composition of  
810 atmospheric oxygen as a tracer of biosphere productivity, *Nature*, 400, 547-550,  
811 <https://doi.org/10.1038/22987>, 1999.

812

813 Malaizé, B., Paillard, D., Jouzel, J., and Raynaud, D.: The Dole effect over the Last two glacial-  
814 interglacial cycles, *J. Geophys. Res.*, 104, 14199-14208, <https://doi.org/10.1029/1999JD900116>,  
815 1999.

816 Mehler, A.: Studies on reactions of illuminated chloroplasts: I. Mechanism of the reduction of  
817 oxygen and other hill reagents, *Arch. Biochem. Biophys.*, 33, 65-77,  
818 [https://doi.org/10.1016/00039861\(51\)90082-3](https://doi.org/10.1016/00039861(51)90082-3), 1951.

819

820 Meijer, H. A. J., and Li, W. J.: The use of electrolysis for accurate  $\delta^{17}O$  and  $\delta^{18}O$  Isotope  
821 Measurements in Water, *Isot. Environ. Health Stud.*, 34, 349-369,  
822 <https://doi.org/10.1080/10256019808234072>, 1998.

823

824 Milcu, A., Allan, E., Roscher, C., Jenkins, T., Meyer, S. T., Flynn, D., Bessler, H., Buscot, F.,  
825 Engels, C., Gubsch, M., König, S., Lipowsky, A., Loranger, J., Renker, C., Scherber, C., Schmid,  
826 B., Thébault, E., Wubet, T., Weisser, W. W., Scheu, S., and Eisenhauer, N.: Functionally and  
827 phylogenetically diverse plant communities key to soil biota, *Ecology*, 94, 1878-1885,  
828 [https://doi.org/ 10.1890/12-1936.1](https://doi.org/10.1890/12-1936.1), 2013.

829

830 Reutenauer, C., A. Landais, A., T. Blunier, T., C. Bréant, C., M. Kageyama, M., M.-N. Woillez, M.-N.,  
831 Risi, C., Mariotti, V., and P. Braconnot, Quantifying molecular oxygen isotope variations during a  
832 Heinrich stadial, *Clim. Past*, 11, 1527-1551, <https://doi.org/10.5194/cp-11-1527-2015>, 2015.

833

834 Ribas-Carbo, M., Berry, J.A., Yakir, D., Giles, L., Robinson, S.A., Lennon, A.M., and Siedow, J.N.:  
835 Electron Partitioning between the Cytochrome and Alternative Pathways in Plant  
836 Mitochondria, *Plant Physiol.*, 109, 829-837, <https://doi.org/10.1104/pp.109.3.829>, 1995.

837

838 Seltzer, A. M., Severinghaus, J. P., Andraski, B. J., and Stonestrom, D. A.: Steady state  
839 fractionation of heavy noble gas isotopes in a deep unsaturated zone, *Water Resour. Res.*, 53,  
840 2716-2732, <https://doi.org/10.1002/2016WR019655>, 2017.

841

842 Severinghaus, J. P., Beaudette, R., Headly, M. A., Taylor, K. and Brook, E. J.: Oxygen-18 of O<sub>2</sub> records  
843 the impact of abrupt climate change on the terrestrial biosphere, *Science*, 324, 1431-1434,  
844 <https://doi.org/10.1126/science.1169473>, 2009.

845

846 Shackleton, N. J.: The 100,000-Year Ice-Age Cycle Identified and Found to Lag Temperature,  
847 Carbon Dioxide, and Orbital Eccentricity, *Science*, 289, 1897-1902,  
848 <https://doi.org/10.1126/science.289.5486.1897>, 2000.

849

850 Sharkey, T.D., Badger, M.R., von Caemmerer, S., and Andrews, T.J.: High Temperature Inhibition of  
851 Photosynthesis Requires Rubisco Activase for Reversibility, *Trends Plant Sci.*, 2465-2468,  
852 [https://doi.org/10.1007/978-94-011-3953-3\\_577](https://doi.org/10.1007/978-94-011-3953-3_577), 1998.

853

854 Sharp, Z. D., and Wostbrock, J. A. G.: Standardization for the Triple Oxygen Isotope System: Waters,  
855 Silicates, Carbonates, Air, and Sulfates, *Rev. Mineral. Geochem.*, 86, 179-196,  
856 <https://doi.org/10.2138/rmg.2021.86.05>, 2021.

857  
858 Stolper, D. A., Fischer, W. W., and Bender, M. L.: Effects of temperature and carbon source on the  
859 isotopic fractionations associated with O<sub>2</sub> respiration for <sup>17</sup>O/<sup>16</sup>O and <sup>18</sup>O/<sup>16</sup>O ratios in *E.*  
860 *coli*, *Geochim. Cosmochim. Ac.*, 240, 152-172, <https://doi.org/10.1016/j.gca.2018.07.039>, 2018.

861 Tcherkez, G., and Farquhar, G.D.: On the <sup>16</sup>O/<sup>18</sup>O isotope effect associated with photosynthetic O<sub>2</sub>  
862 production, *Funct. Plant Biol.*, 34, 1049-1052, <https://doi.org/10.1071/FP07168>, 2007.

863 Tcherkez, G., Gauthier, P., Buckley, T.N, Bush, F.A., Barbour, M.M., Bruhn, D., Heskell, M.A., Gong, X.Y.,  
864 Crous, K.Y., Griifin, K., Way, D., Turnbull, M., Adams, M.A., Atkin, O.K., Farquhar, G.D., and Cornic, G.:  
865 Leaf day respiration: low CO<sub>2</sub> flux but high significance for metabolism and carbon balance, *New*  
866 *Phytol.*, 216, 986-1001, <https://doi.org/10.1111/nph.14816>, 2017.

867 Vinogradov, A. P., Kutyurin, V.M., and Zadorozhnyi, I.K.: Isotope fractionation of atmospheric oxygen,  
868 *Geochem. Int.*, 3, 241-253, 1959.

869 Wang, Y., Cheng, H., Lawrence Edwards, R., Kong, X., Shao, X., Chen, S., Wu, J., Jiang, X., Wang, X.,  
870 and An, Z.: Millennial- and orbital-scale changes in the East Asian monsoon over the past 224,000  
871 years, *Nature*, 451, 1090-1093, <https://doi.org/10.1038/nature06692>, 2008.